Electronic Supplementary Material (ESI) for Dalton Transactions.

Supporting information

PbX_2(OOCMMIm) (X = Cl, Br): Photoluminescent Organic-inorganic Hybrid Lead Halide Compounds with High Proton Conductivity

Liao-Kuo Gong[a,c], Ke-Zhao Du*[b] and Xiao-Ying Huang*[a]

[a] *State Key Laboratory of Structure Chemistry, Fujian Institute of Research on the Structure of Matter, Chinese Academy of Sciences, Fuzhou 350002, China.*

[b] *College of Chemistry and Materials Science, Fujian Normal University, 32 Shangsan Road, Fuzhou 350007, China.*

[c] *University of Chinese Academy of Sciences, Beijing, 100049, China.*

† E-mail: xyhuang@fjirsm.ac.cn; duke@fjnu.edu.cn

Table of Contents

Experimental Section

Materials

1-carboxymethyl-3-methylimidazolium halides ([HOOCMMIm]*X*; *X* = Cl, Br) (99%) were purchased from Lanzhou Yulu Fine Chemical Co., LTD (Lanzhou, China); lead halides (PbX_2, *X* = Cl, Br) (99.0%) were purchased from Beijing HWRK Chem Co., LTD (Beijing, China); N,N′-dimethyl formamide (DMF, 99.0%) was purchased from Sinopham Chemical Reagent Co., Ltd. (Shanghai, China). All the chemicals were used without further purification.

Synthesis

Growth of [PbX_2(OOCMMIm)] (*X* = Cl for **1**, Br for **2**) crystals. A mixture of [HOOCMMIm]*X* (*X* = Cl for **1**, Br for **2**) and PbX_2 (*X* = Cl for **1**, Br for **2**) with the molar stoichiometric ratio of 2:1 in DMF was loaded into a 28 mL Teflon-lined stainless steel autoclave. The container was closed and heated at 140 °C for 6 days, and then cooled to room temperature naturally, resulting in a homogeneous brown solution. Colourless block-like crystals were obtained by filtration and dried in air naturally.

Characterization methods

Single crystal X-ray diffraction (SCXRD). A suitable single crystal was carefully selected under an optical microscope and glued to a thin glass fiber. The single-crystal X-ray diffraction data were collected on a SuperNova CCD diffractometer with graphite-monochromated MoKα radiation (λ = 0.71073 Å) at 100(2) K. The structures were solved by direct methods and refined by full-matrix least-squares on F^2 using the SHELXL-2016 program package.[1] All non-hydrogen atoms were refined anisotropically. Hydrogen atoms attached to C atoms were located at geometrically calculated positions and were not refined. CCDC 1902685 for compound **1** and CCDC 1902686 for compound **2** contain the supplementary crystallographic data for the two structures.

Powder X-ray diffraction (PXRD). PXRD was measured on a Rigaku Miniflex-II diffractometer with Cu $K\alpha$ radiation (λ = 1.54178 Å) in the angular range of 2θ = 3-65° with a scan speed of 2°/min. The simulated PXRD patterns are based on single-crystal X-ray diffraction data using the Mercury program.[2]

Elemental analysis (EA). EA was performed using a German Elementary Vario EL III instrument.

Thermogravimetric analysis (TGA). TGA was performed on a NETZSCH STA 449F3 unit at a heating rate of 10 K·min^{-1} under N_2 atmosphere.

Solid state optical adsorption spectra. Solid state diffuse reflectance spectra were recorded at room temperature using Shimadzu 2600 UC/Vis spectrometer in the range of 800~200 nm with a $BaSO_4$ plate as a reference (100% reflectance). The adsorption data were calculated from the diffuse reflectance using the Kubelka-Munk function $\alpha/s = (1-R)^2/2R$. Where α is the adsorption coefficient; S is the scattering coefficient and R is the diffuse reflectance.

Proton conduction measurements. AC impedance measurements were carried out with a SI 1260 IMPEDANCE/GAINPHASE analyzer over the frequency range from 0.1 Hz to 1M Hz with an applied voltage of 100 mV. The relative humidity was controlled by a STIKCorp CIHI-150BS3 incubator. The samples were pressed into a cylindrical pellet of crystalline powder sample (~1.4 mm thickness ×5 mm Φ for **1** and ~1.8 mm thickness ×5 mm Φ for **2**) coated with silver colloid. Two silver electrodes were attached to both sides of pellet to form four end terminals (quasi = four-probe method). The bulk conductivity was estimated by semicircle fittings of Nyquist plots.

Photophysical properties. PL (photoluminescence), PLE (photoluminescence excitation) and TRPL (time-resolved photoluminescence) were recorded on an Edinburgh FL980 UV/V/NIR fluorescence spectrometer. Quantum yields were measured by Edinburgh FLS 1000 UV/V/NIR fluorescence spectrometer.

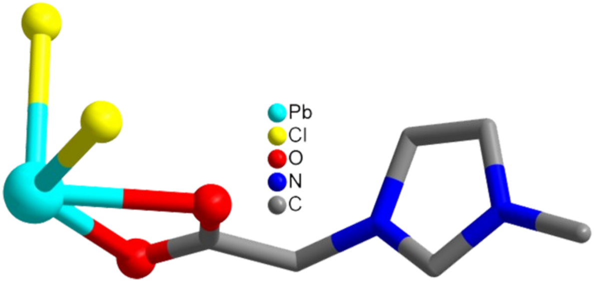

Fig. S1 The asymmetric unit of [PbCl(OOCMMIm)] (**1**).

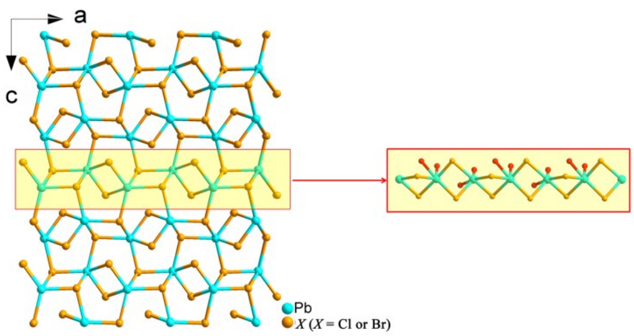

Fig. S2 The structure of PbX_2 (left) and the 1D chain in [PbX_2(OOCMMIm)] (right) (X = Cl, Br).

Table S1. Crystallographic data and refinement details for compounds1 and 2.

Crystal	[Pb(OOCMMIm)Cl_2] (**1**)	[Pb(OOCMMIm)Br_2] (**2**)
Empirical formula	$C_6H_8Cl_2N_2O_2Pb$	$C_6H_8Br_2N_2O_2Pb$
Formula weight	418.23	507.15
Crystal system	$P2_1/c$	$P2_1/c$
Space group	monoclinic	monoclinic
a/Å	8.0984(6)	8.3012(4)
b/Å	17.9704(10)	18.5784(7)
c/Å	7.8257(6)	7.9673(3)
β/°		
V/Å^3	1052.61(14)	1129.74(9)
Z	4	4
T/K	295	298
F(000)	760.0	904
ρ_{calcd}/g cm^{-3}	2.639	2.982
μ/mm^{-1}	16.505	21.980
Measured refls.	5633	8763
Independent refls.	2193	2659
No. of parameters	120	119
R_{int}	0.0261	0.0551
R_1 ($I > 2\sigma(I)$)[a]	0.0326	0.0429
wR ($I > 2\sigma(I)$)[b]	0.0819	0.0795
GOF	0.999	1.014

[a] $R_1 = \sum \| F_o| - |F_c \| / \sum |F_o|$, [b] $wR_2 = [\sum w(F_o^2 - F_c^2)^2 / \sum w(F_o^2)^2]^{1/2}$.

Table S2 Hydrogen bonding data for compounds 1 and 2.

1

D-H---A	d(H---A) (Å)	d(D---A) (Å)	d(D-H) (Å)	< (DHA) (°)
C(2)-H(2A)---Cl(1)#3	2.62	3.529(8)	0.97	155.6
C(2)-H(2B)---Cl(1)#4	2.86	3.739(8)	0.94	151.5
C(3)-H(3A)---Cl(2)#5	2.77	3.452(9)	0.93	131.3
C(4)-H(4A)---Cl(1)#6	2.95	3.613(9)	0.93	129.3
C(5)-H(5A)---Cl(1)#7	2.88	3.487(8)	0.93	123.8
C(5)-H(5A)---O(1)#1	2.35	3.049(10)	0.93	132.0

Symmetry transformations used to generate equivalent atoms: #1 $x,-y+1/2,z+1/2$; #2 $x,-y+1/2,z-1/2$; #3 $x+1,-y+1/2,z+1/2$; #4 $x+1,y,z$; #5 $-x+1,-y+1,-z+1$; #6 $-x+1,-y+1,-z+2$; #7 $x+1,y,z+1$

2

D-H---A	d(D-H) (Å)	d(H---A) (Å)	d(D---A) (Å)	< (DHA) (°)
C(2)-H(2A)---Br(1)#3	0.97	2.77	3.634(8)	148.6
C(2)-H(2B)---Br(1)#4	0.97	2.91	3.851(8)	163.4
C(3)-H(3A)---Br(2)#5	0.93	3.03	3.626(10)	123.3
C(4)-H(4A)---Br(1)#6	0.93	3.07	3.762(9)	132.6
C(5)-H(5A)---Br(1)#7	0.93	3.08	3.589(8)	116.3
C(6)-H(6A)---Br(2)#6	0.96	3.20	3.612(9)	107.8
C(5)-H(5A)---O(1)#1	0.93	2.36	3.106(10)	136.7

Symmetry transformations used to generate equivalent atoms: #1 $x,-y+1/2,z+1/2$; #2 $x,-y+1/2,z-1/2$; #3 $x+1,-y+1/2,z+1/2$; #4 $x+1,y,z$; #5 $-x+1,-y+1,-z+1$; #6 $-x+1,-y+1,-z+2$; #7 $x+1,y,z+1$

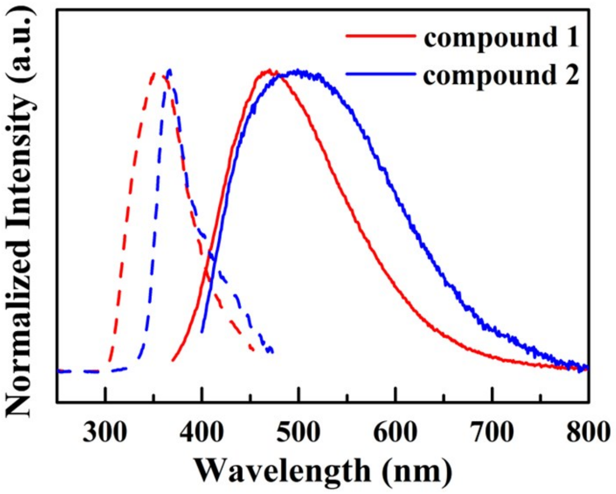

Fig. S3 Solid state excitation (dashed lines) and emission (solid lines) spectra for **1** and **2** at room temperature (λ_{ex} = 350 nm and λ_{em} = 470 nm for **1**, λ_{ex} = 365 nm and λ_{em} = 500 nm for **2**).

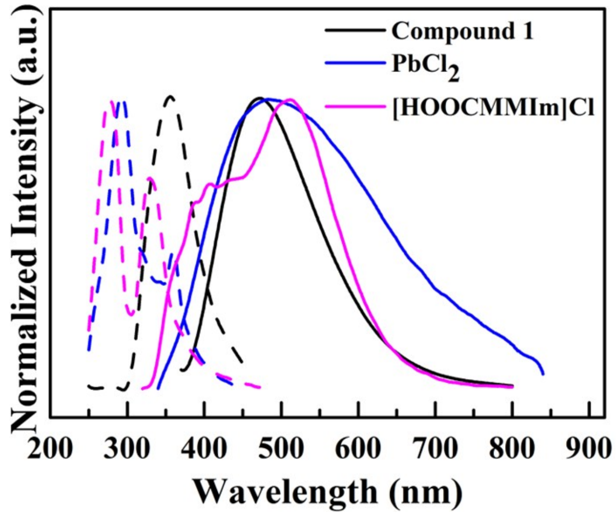

Fig. S4 Fluorescence spectra of compound **1** (λ_{ex} = 350 nm, λ_{em} = 470 nm), $PbCl_2$ (λ_{ex} = 295 nm, λ_{em} = 480 nm) and [HOOCMMIm]Cl (λ_{ex} = 280 nm, λ_{em} = 512nm).

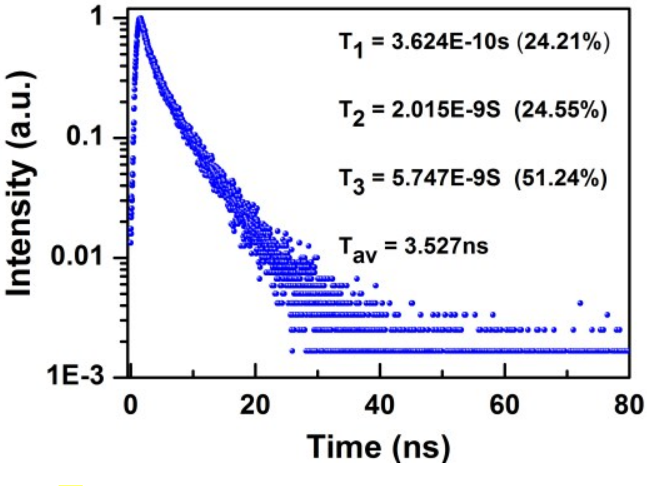

Fig. S5 The fluorescence decay time spectrum of compound **1**.

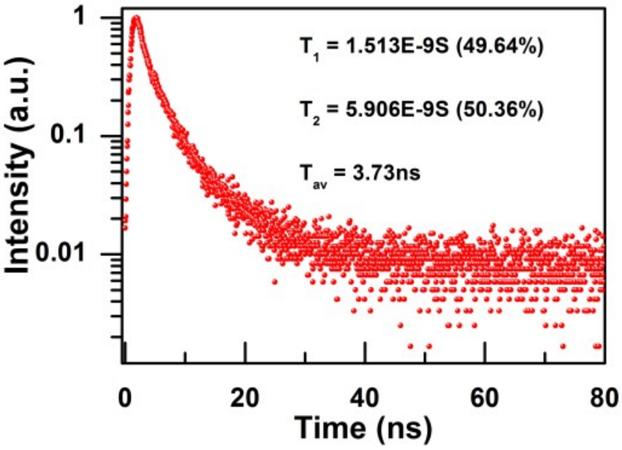

Fig. S6 The fluorescence decay time spectrum of compound **2**.

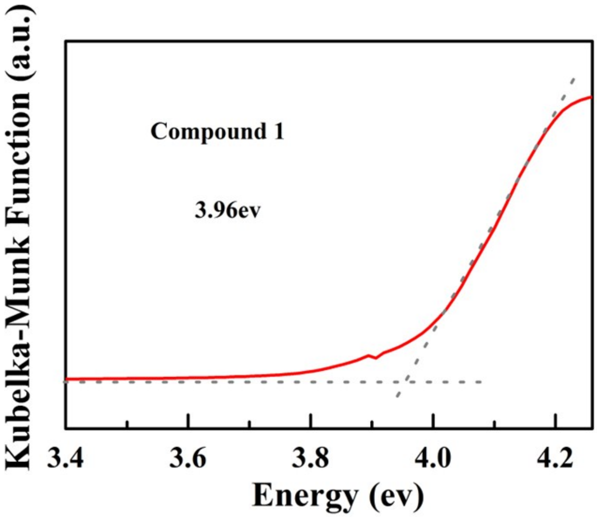

Fig. S7 UV-Vis spectrum of compound **1**.

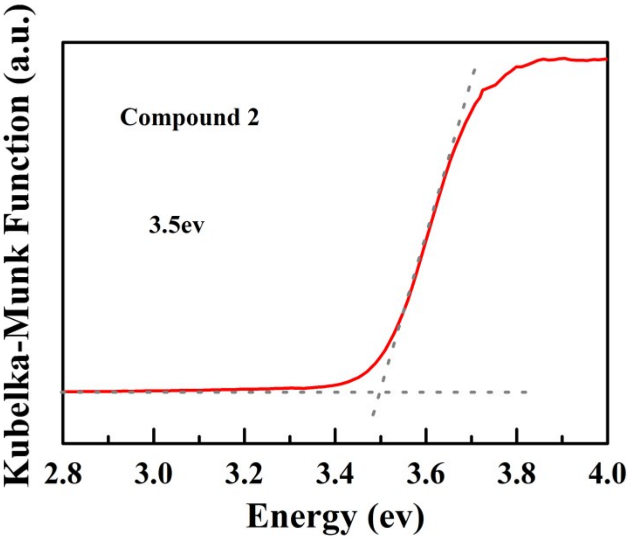

Fig. S8 UV-Vis spectrum of compound **2**.

Photoluminescence properties for compounds 1 and 2

Besides the proton conduction, the title compounds also exhibit interesting photoluminescence (PL). As shown in Fig. S3, under optimal excitations (350 nm for **1** and 365 nm for **2**), compounds **1** and **2** exhibit blue-green and yellow broad emissions peaking at 470 nm (CIE (0.229, 0.291)) and 500 nm (CIE (0.451, 0.461)), respectively. The quantum yields (*QY*s) are characterized as 4.79% for **1** and 2.79% for **2**, respectively, which can be compared with that of reported metal halides.[3-6] The decay times of **1** and **2** are 3.53 ns and 3.73 ns, respectively. To better understand the photoluminescence mechanism, the emissions of [HOOCMMIm]Cl and bulk $PbCl_2$ were investigated. As shown in Fig. S4, $PbCl_2$ displays a blue light emission centred at ~480 nm under 295 nm excitation, whereas [HOOCMMIm]Cl shows a blue light emission centred at 512 nm under 280nm excitation. The range of these emissions overlap with that of **1**, demonstrating that blue-green emission in **1** is derived from the synergetic contribution of inorganic and organic parts.[5, 7] The PL of **2** exhibits a red shift compared with that of **1**, which should be due to the narrower bandgap of **2** as shown in Figs. S7 and S8. The wide peaks should arise from the self-trapping exciton induced by the lattice distortion of the octahedron (PbX_4O_2) in the structures.[3,4]

Table S3 Comparison of the photoluminescent data of title compounds and the reported ones.

Compound	*QY*	λ_{ex}, λ_{em}(nm)	Ref.
[$PbCl_2$(bp4mo)] (bp4mo = N-oxide-4,4'-bipye)	6%	380, 600	6
[$PbBr_2$(bp4mo)] (bp4mo = N-oxide-4,4'-bipye)	22%	380, 600	6
$[Pb_2F_2][O_2C(CH_2)_4CO_2]$	1.8%	280, 541	4
$[Pb_2Cl_2][O_2C(CH_2)_4CO_2]$	11.8%	327, 536	4
$[Pb_2Br_2][O_2C(CH_2)_4CO_2]$	2%	356, 565	4
$[PbBr_2][O_2C(CH_2)_4CO_2]$	5.6%	360, 530	3
$[Pb_3Br_4][O_2C(CH_2)_2CO_2]$	1.8%	370, 480	3
[$PbCl_2$(OOCMMIm)]	4.79%	350, 470	This work
[$PbBr_2$(OOCMMIm)]	2.79%	365, 500	This Work

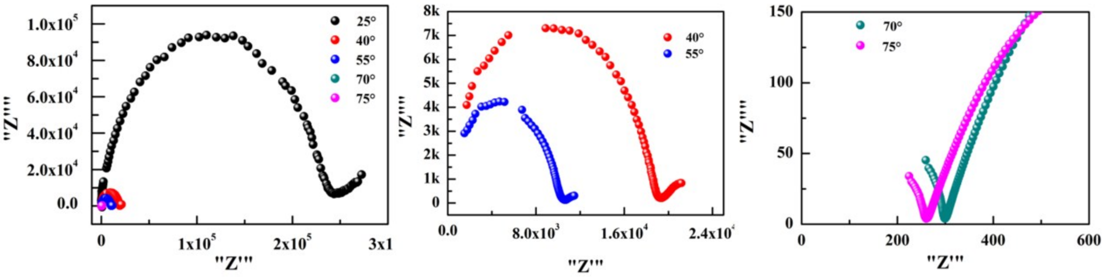

Fig. S9 Impedance spectra of compound **2** at 98% RH and different temperatures.

Reference:

1. G. M. Sheldrick, *Acta Crystallogr. Sect. C* 2015, **71**, 3-8.
2. http://www.ccdc.cam.au.uk/mercury/
3. C. Peng, Z. Zhuang, H. Yang, G. Zhang and H. Fei, *Chem. Sci.*, 2018, **9**, 1627-1633.
4. Z. W. Zhuang, C. D. Peng, G. Y. Zhang, H. M. Yang, J. L. Yin and H. H. Fei, *Angew. Chem. Int. Ed.*, 2017, **56**, 14411-14416.
5. G.-E. Wang, G. Xu, M.-S. Wang, L.-Z. Cai, W.-H. Li and G.-C. Guo, *Chem. Sci.*, 2015, **6**, 7222-7226.
6. O. Toma, N. Mercier, M. Allain, F. Meinardi and C. Botta, *Eur. J. Inorg. Chem.*, 2017, **2017**, 844-850.
7. L. L. Zhu, Y. E. Huang, Y. P. Lin, X. Y. Huang, H. Q. Liu, D. B. Mitzi and K. Z. Du, *Polyhedron*, 2019, **158**, 445-448.